

**Title of the project:**

**Design of quasi-3D integrated lens antennas**

**Applicant**

Dr. **Artem V. BORISKIN**  
Institute of Radiophysics and Electronics (IRE)  
National Academy of Sciences of Ukraine (NASU)  
12, Acad. Proskury Str., Kharkiv 61085, Ukraine  
[a\\_boriskin@yahoo.com](mailto:a_boriskin@yahoo.com)

**Host**

Prof. **Ronan SAULEAU**  
IETR, Groupe Antennes et Hyperfréquences  
Université de Rennes 1 – Campus de Beaulieu  
Tel: 02 23 23 56 76  
[Ronan.Sauleau@univ-rennes1.fr](mailto:Ronan.Sauleau@univ-rennes1.fr)

**Duration of the stay**

**6 months** (September 2010 until February 2011)

**Purpose of the visit**

The purpose of the visit was to stimulate the on-going research on the development of synthesis-oriented CAD tools based on the rigorous analytical methods, namely: the exact series expansion (SE) methods for the radially-symmetrical lenses and Muller’s Boundary Integral Equations (MBIE) in combination with the Method of Analytical Regularization (MAR) for arbitrary shaped ones.

**Description of the work & main results obtained**

The research carried out during the exchange period covered the following three directions:

1. CAD development,
2. Design and optimization of multi-shell radially-symmetrical lens antennas,
3. Design and optimization of arbitrary-shaped lens antennas.

The description of each work-package (WP) and the corresponding results obtained are given below.

## WP-1: CAD development

The goal of this WP was to develop advanced global optimization algorithms, suitable for fast and reliable optimization of multi-parameter and multi-extremum functions, and to merge them with recently developed electromagnetics (EM) solvers based on the exact SE [1] and MBIE/MAR [2,3] techniques for radially-symmetric and arbitrary-shaped lenses, respectively.

To meet this challenge a Hybrid Genetic Algorithms (HGA) has been developed base on a combination of a binary GA and steepest descent gradient (SDG) algorithms (Fig. 1). The algorithm uses the inherent skills of the GA for global exploration (enhanced by an appropriate choice of the selection and reproduction schemes and rates) and the gradient-based down-hill movement for local search. A distinctive feature of the proposed algorithm is that it aims not only at the very best solution but also identifies a given number of next-to-the-best solutions to be then investigated with the aid of the gradient-based optimizer. Such a two-step approach enables us to significantly reduce the GA stagnation period at the later stage of optimization and to assure achievement of the very bottom of all the identified extrema. The latter helps to collect the problem-specific information that is then incorporated in code in the form of specific encoding schemes best suited for the addressed problem. Finally, the speedup is achieved by creating a stack which holds parameters of the already known individuals and corresponding values of the fitness function.

The developed algorithm was first approbated on the linear array synthesis problem (Figs. 2 and 3) and than merged with the available EM solvers based on the SE [1] and MBIE/MAR [2,3] techniques. More details about HGA are given in Ref. [4].

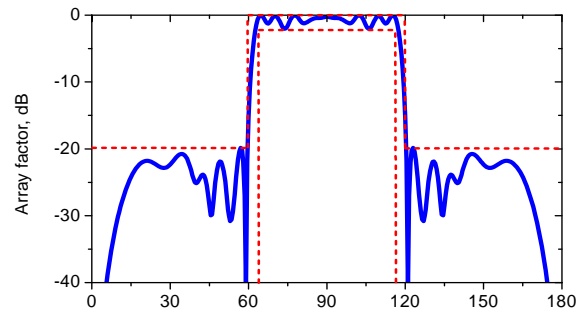
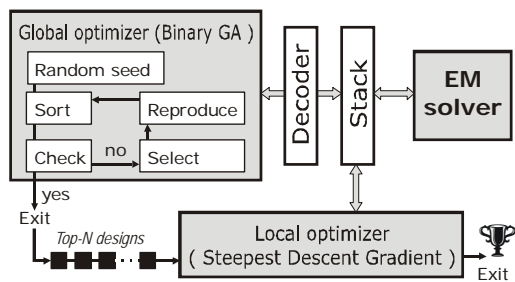


Fig. 1. Flowchart of the hybrid genetic algorithm.

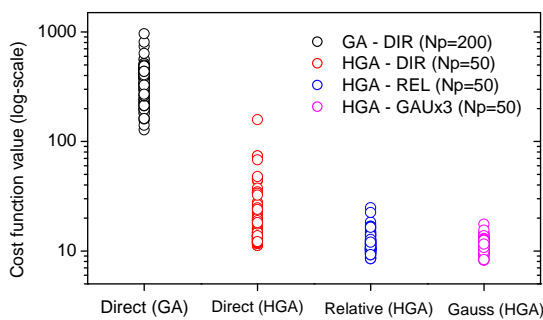


Fig. 2. Best solutions (100 independent runs) found by standard GA and HGA with three different encoding schemes when applied for a linear array synthesis problem – see Fig. 3. Population size for GA and HGA algorithms is 200 and 50 individs, respectively. Stop condition for both algorithms is 50 iterations. The significant advantage of HGA vs. classical GA in terms of both solution quality and stability in hitting the global extrema is demonstrated.

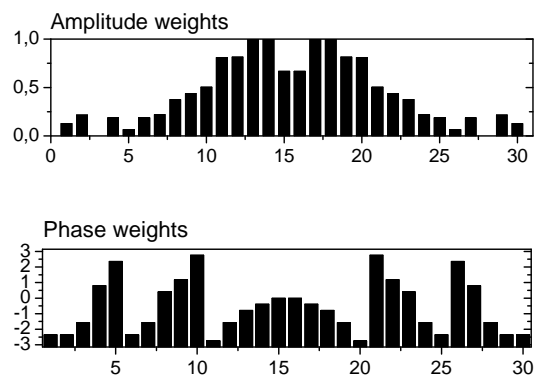


Fig. 3. Array factor of the symmetrical linear array of 30 elements spaced  $\lambda/2$  apart with optimized phase and amplitude weights.

## WP-2: Design and optimization of multi-shell radially-symmetrical lenses

The goal of this WP was to define the optimal configuration of a multi-shell discrete Luneburg lens (LL) and to provide insight into the design of its low-cost analogs.

To solve this problem a new synthesis-oriented CAD tool has been developed as a combination of the SE-based solver [1] and the new HGA optimization algorithm [4]. High efficiency of the new software in terms of accuracy and resources consumption enabled us to perform a systematic study of the multi-shell Luneburg lenses (LL) of different sizes and made of various dielectric materials.

### Problem formulation

For numerical analysis, we consider uniformly-layered multi-shell LL [5], and two-shell lens with radius  $R_M = 5, 10$  and  $15\lambda_0$  ( $M$  is number of layers). For the latter, the core is assumed to be made of standard low permittivity materials, such as Teflon ( $\varepsilon = 2.1$ ), Rexolite ( $\varepsilon = 2.53$ ), Fused Silica ( $\varepsilon = 3.27$ ), and Quartz ( $\varepsilon = 3.8$ ), and the outer shell of arbitrary dielectric materials whose permittivity is below the one of the core material. As possible candidates for the outer shell, Polyurethane foam (PUF,  $\varepsilon = 1.2$ ) and Teflon are considered. All materials are assumed to be isotropic and lossless. Thickness of the air-gap between the shells is controlled by parameter  $\Delta$  (Fig. 4).

The feed is modelled by a complex-source point (CSP) beam [6]. In simulations, CSP is located at a fixed distance from the lens surface ( $\delta = \lambda_0/10$ ), and its beam waist parameter  $kb$  equals 3.0 ( $k = 2\pi/\lambda_0$ ) that corresponds to the full half-power beamwidth of  $36^\circ$ . The selection of these parameters is justified in [7].

### Results obtained

- The optimal excitation conditions for multi-shell LL have been defined. As was shown the general -10 dB edge illumination rule well suited for large-size multi-shell lenses, should be changed for two-shell lenses in the favor of a lower value depending on the core size [7].
- A low-cost analogs of a multi-shell discrete LL are presented based the optimized two-shell designs. As demonstrated, properly designed two-shell lenses made of standard low-permittivity dielectric materials can provide nearly the same directivity as multi-shell LLs, provided the shell thickness is properly defined with respect to the materials permittivity (Figs. 5,6). Unlike earlier studies [5], the proposed two-shell lenses are based on low-permittivity materials that makes them lighter and less affected by internal resonances. The numerical data, computed for lenses of different size and material in many simulation cycles, have been organized in a chart enabling one to determine the optimal parameters of two-shell lenses made of arbitrary dielectric materials without solving the corresponding diffraction problems (Fig. 7). The validity of the outlined recommendations is proven by the excellent agreement with experimental and numerical data reported by other authors.
- The impact of the air-gap size on the LL collimating characteristics has been carefully studied. As shown, air gaps enhance resonant effects that can lead to significant directivity degradation in narrow bands around the resonant frequencies [8].
- Finally, the influence of whispering gallery modes (WGM) on the focusing and collimating characteristics of LLs has been accurately described (Fig. 8). As demonstrated, WGMs can arise at the periphery and inner boundaries both in emitting and receiving modes. Their excitation is accompanied by drops in the antenna directivity due to increase of dissipation losses and resonant scattering. The impact of WGMs grow versus the contrast at the boundaries and can be especially strong (e.g. directivity loss over 20%) for lenses with a few shells, dense core and/or those having air-gaps between layers [8].

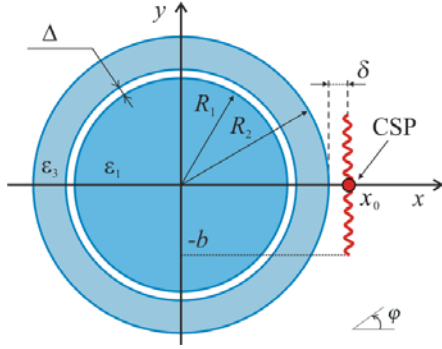


Fig. 4. Geometry and notations of the problem. The lens is illuminated by a CSP feed located at a certain distance from the lens surface and oriented to radiate in the negative  $x$  direction. The curve line indicates the branch cut in real space due to CSP.

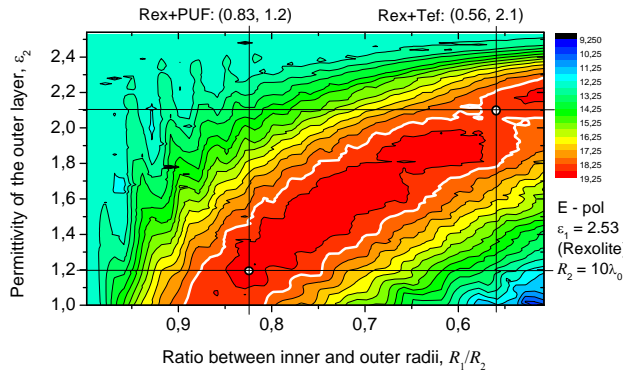


Fig. 5. Broadside directivity (color bar, dB scale) of the E-polarized CSP feed assisted by a two-shell Rexolite-core lens ( $\Delta = 0$ ,  $R_2 = 10\lambda_0$ ) vs. ratio between the inner and outer shells radii and the outer shell permittivity.

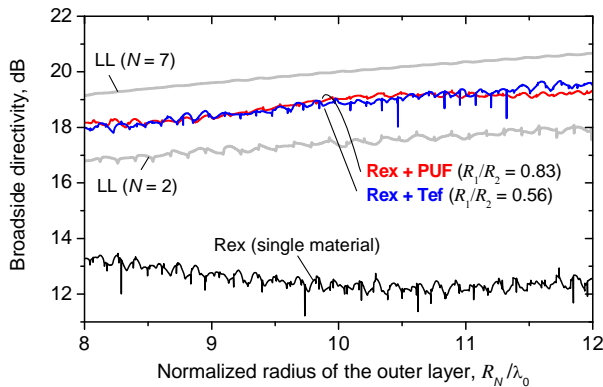


Fig. 6. Broadside directivity of the CSP feed assisted by the uniformly-layered LLs (made of two and seven layers) and their low-cost analogs, i.e. a single-material lens and optimized two-shell lenses with cores made of Rexolite and outer shells made of PUF and Teflon, respectively. Parameters of the optimized lenses correspond to the marks in Fig. 5.

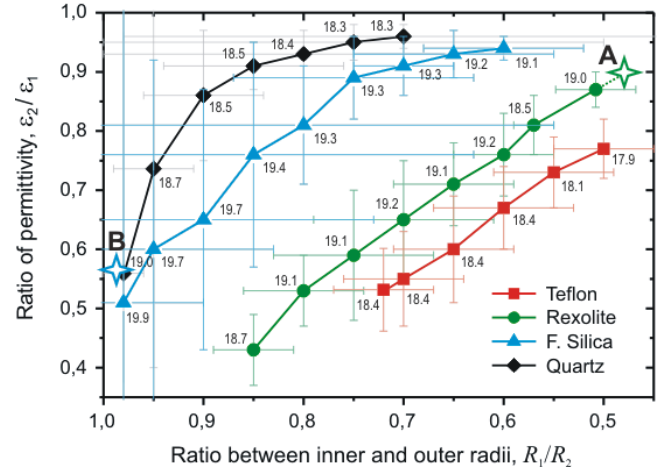


Fig. 7. Cumulative chart representing the optimal pairs of relative parameters (radii and permittivity) for lenses with  $R_2 = 10\lambda_0$  and cores made of different materials (see legend). The corresponding directivity values are shown near each mark. The error bars indicate the range of parameters that guarantees deviation of the directivity value from its peak value for not more than 1 dB (see the white contour line in Fig. 5). The star marks correspond to the designs reported by other authors: (A) Rexolite-Polyethylene ( $\epsilon_2 = 2.25$ ) lens with  $R_1/R_2 = 0.47$  – Refs. [9,10] and (B) synthesized two-shell lens made of two arbitrary materials ( $\epsilon_1 = 3.29$ ,  $\epsilon_2 = 1.87$ ) with  $R_1/R_2 = 0.98$  – Ref. [5]. The color of stars corresponds to the core material permittivity value.

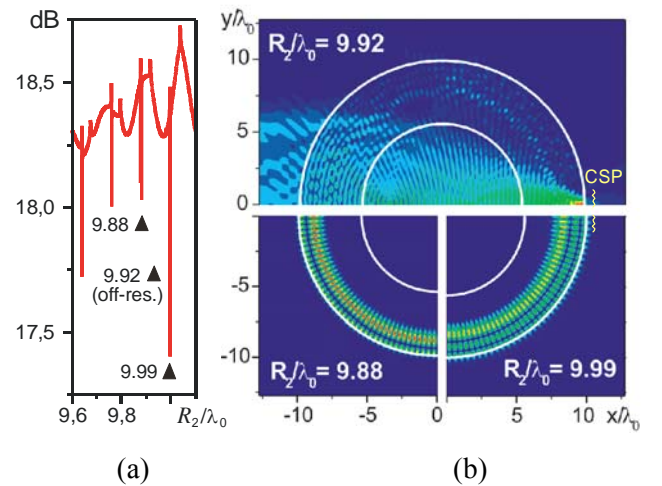


Fig. 8. (a) Zoom of Fig. 6 for Rex + Tef. lens, (b) Normalized near-field maps of the lenses with resonant and non-resonant dimensions – see triangular marks in (a). Due to symmetry, only parts of the maps are shown: upper half for the non-resonant case and lower quarters for the resonant ones.

### WP-3: Design and optimization of arbitrary-shaped lenses

The goal of this WP was to pave the way for design of shaped planar dielectric slab lens antennas for beam-switching applications.

To fulfill this task a new synthesis-oriented CAD tool has been developed by merging the MBIE/MAR solver [2,3] and the new HGA optimization algorithm [4]. The main advantages of the developed tool are: (i) time/memory efficiency and controlled accuracy for any set of geometrical and physical parameters intrinsic to the MBIE/MAR solver and (ii) capability of fast and reliable search for the global extrema of multi-parameter cost-functions characterizing the radiation characteristics of the lens antennas provided by the HGA.

The work included accurate characterization of conventionally-shaped dielectric lens antennas (DLAs) considered as a reference solution and synthesis of shaped DLAs fed by focal arrays.

#### Problem formulation

As we aim at the development of quasi-3D lens antennas (with planar dielectric slab lenses whose thickness is smaller than the wavelength in lens material [11]), an effective index approach [12] can be applied to reduce dimensionality of the problem. Thus we consider the problem in two-dimensional formulation and model the lens by a homogeneous dielectric cylinder whose contour is defined by a given number of spline nodes. For conventionally-shaped hemielliptic and hemispherical lenses the shape is defined with respect of the optical focusing rule [13], whereas for shaped lenses positions of nodes serve as parameters of optimization (Fig. 9).

A plane wave and CSP feed(s) [6] are used to excite the antenna operating in receiving and emitting modes, respectively. Note that imaginary part of the CSP coordinate determines the waist of the CSP beam that makes CSP a convenient (compact-form) model of an aperture feed [4]. In computations, CSP feeds are located outside the lens close to its flat bottom ( $\delta = \lambda_0/10$ ) and oriented to radiate in the opposite  $x$ -axis direction. Parameters of the feeding array included in optimization: feeds locations along  $y$ -axis ( $d_i$ ) and beam-width parameters ( $b_i$ ). The array is assumed to be symmetrical with respect to the  $x$ -axis, so only  $(N/2+1)$  feeds are considered, where  $N$  is the number of elements in the feeding array. The reference solution is computed for the extended hemielliptic lens made of the same material and having the same flat-bottom size. The beam directions for the shaped lens fed by an optimized focal array are defined to be the same as those computed for the hemielliptic DLA fed by a uniformly-spaced array.

#### Results obtained

- Accurate characterization of the focusing and collimating characteristics of hemielliptical and hemispherical lenses made of various materials (Figs. 10, 11). As demonstrated, such lenses support half-bowtie resonances that can strongly affect performance of integrated lens antennas (ILAs). The resonant properties of compact-size lenses can become dominant already for lenses made of materials with permittivity  $\epsilon > 4$  (Fig. 11). More details are given in [14].
- Demonstration of the principle possibility for the design of shaped flat-bottom lenses with improved angular characteristics. For the test-case antenna (i.e. Rexolite lens with bottom size of  $6\lambda_0$  fed by a focal array of 5 feeds) the directivity degradation for off-axis feeds has been reduced to less than 10% in contrast to over 25% observed for the conventional hemielliptic lens of the same size and material (Fig. 12). The relative advantage in absolute values of feeds directivity compared to the reference solution achieved roughly 12%, 30%, and 38% for the central and offset feeds, respectively. As seen in Fig. 13, this advantage is gained thanks to sharpening of main-lobes as well as reduction of the side-lobe level. More details about synthesis of shaped planar slab lens antennas will be given in a forthcoming paper.

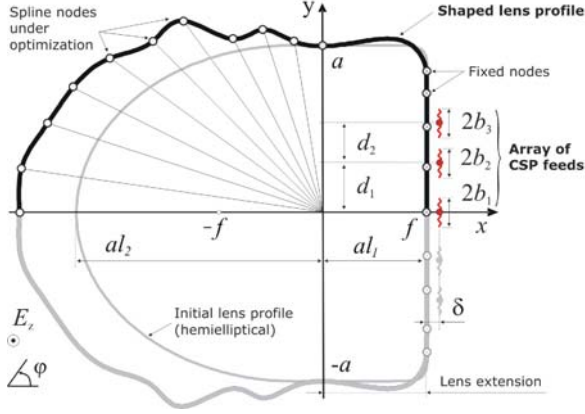


Fig. 9. Geometry and notations of a 2-D model of the shaped planar slab DLA fed by a focal array. Lens profile is defined using cubic splines. The lens is symmetric with respect to  $x$ -axis (the mirrored part is shown in grey color). Curvy lines show the branch cuts associated with CSP feeds.

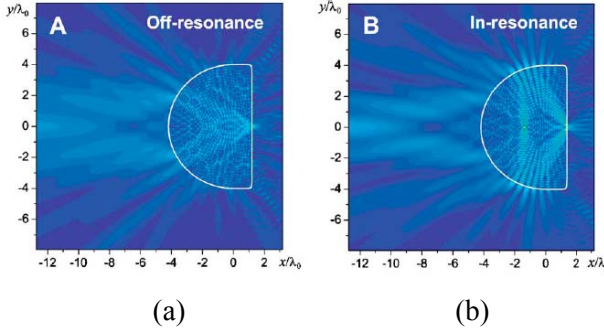


Fig. 10. Normalized near-field maps of a silicon hemielliptical lens excited by a CSP feed: (a) Non-resonant (focusing), (b) resonant (HBT modes) near-fields of the silicon EHE lens.

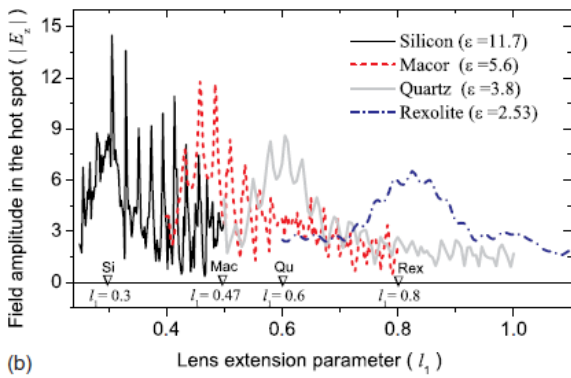


Fig. 11. Interplay between the optical focusing and resonant mechanisms in the near-field enhancement for extended hemielliptical lenses ( $\varnothing=6\lambda_0$ ) made of different materials (see legend). The lenses are illuminated by the unit-amplitude E-polarized plane waves. The marks at the bottom axis indicate the extension values provided by the GO focusing rule.

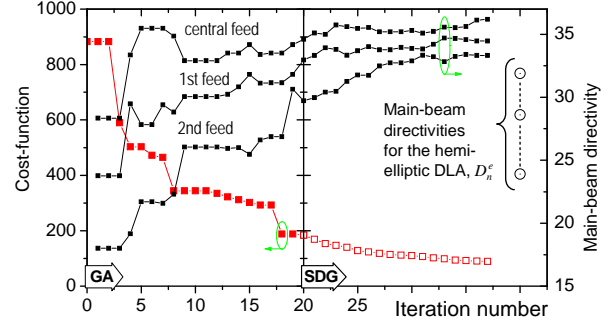


Fig. 12. Optimization process: cost-function (left) and main-beam directivity for each feed (right) vs. number of iteration of the optimization routine. The three curves associated with the right axis indicate directivities of three independent feeds of the focal array when assisted by the shaped lens. The reference values of the main-beam directivities for the hemielliptical DLA,  $D_{i0}^*$  are indicated by hollow circles on the right side.

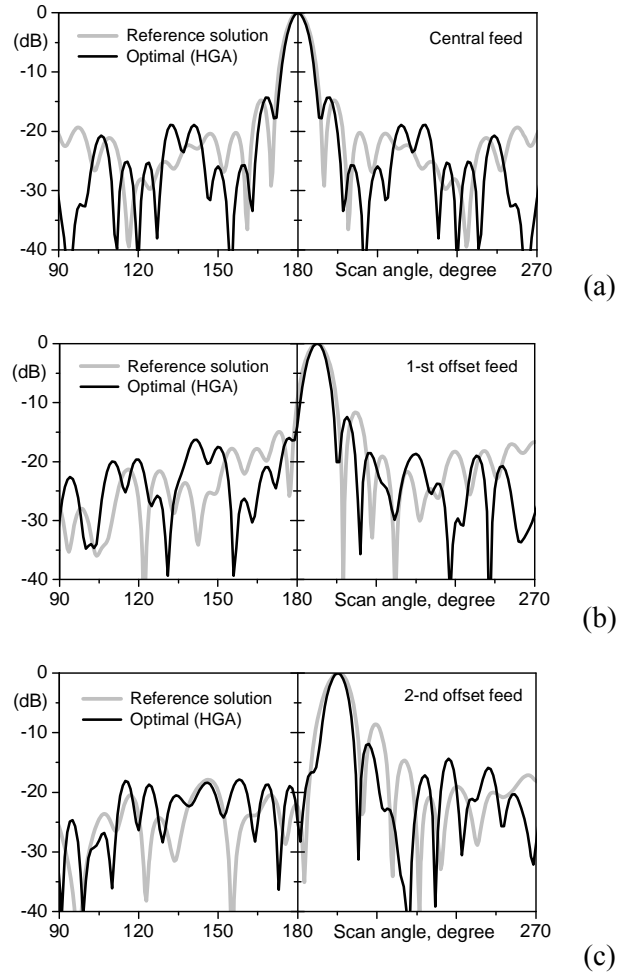


Fig. 13. Normalized radiation patterns for each feed of the CSP array assisted by the shaped (black line) and hemielliptical (grey line) lenses.

## References

- [1] A.V. Boriskin and A.I. Nosich, "Whispering-gallery and Luneburg-lens effects in a beam-fed circularly-layered dielectric cylinder," *IEEE Trans. Antennas Propag.*, vol. AP-50, no. 9, pp. 1245–1249, Sep. 2002.
- [2] A.V. Boriskin, G. Godi, R. Sauleau, and A.I. Nosich, "Small hemielliptic dielectric lens antenna analysis in 2-D: boundary integral equations versus geometrical and physical optics," *IEEE Trans. Antennas Propag.*, vol. 56, no. 2, pp. 485–492, Feb. 2008.
- [3] A.V. Boriskin, A. Rolland, R. Sauleau, and A.I. Nosich, "Assessment of FDTD accuracy in the compact hemielliptic dielectric lens antenna analysis," *IEEE Trans. Antennas Propag.*, vol. 56, no. 3, pp. 758–764, Mar. 2008.
- [4] A.V. Boriskin, M.V. Balaban, A.Yu. Galan, and R. Sauleau, "Efficient approach for fast synthesis of phased arrays with the aid of a hybrid genetic algorithm and a smart feed representation," *IEEE Int. Symp. Phased Array Systems and Tech. (ISPAST)*, Boston (USA), Oct. 2010, pp. 827–832.
- [5] H. Mosallaei and Y. Rahmat-Samii, "Nonuniform Luneburg and two-shell lens antennas: radiation characteristics and design optimization," *IEEE Trans. Antennas Propag.*, vol. 49, no. 1, pp. 60–69, Jan. 2001.
- [6] E. Heyman and L.B. Felson, "Gaussian beam and pulsed-beam dynamics: complex-source and complex-spectrum formulations within and beyond paraxial asymptotics," *J. Opt. Soc. Am. A*, vol. 18, no. 7, pp. 1588–1611, 2001.
- [7] A.V. Boriskin, A. Vorobyov, and R. Sauleau, "Two-shell radially symmetric dielectric lenses as low-cost analogs of the Luneburg lens," *IEEE Trans. Antennas Propag.*, vol. 59, 2011 (accepted, in press).
- [8] A.V. Boriskin and R. Sauleau, "Collimating and resonant properties of two-shell radially symmetric lenses," *Proc. 5th European Conf. Antennas Propag. (EuCAP)*, Rome (Italy), 2011 (ID 1569370037).
- [9] D. Gray, J. Thornton, and R. Suzuki, "Assessment of discretised Sochacki lenses," *Loughborough Antennas Propag. Conf. (LAPC)*, Nov. 2009, pp. 289–300.
- [10] J. Thornton, A. White, and D. Gray, "Multi-beam lens-reflector for satellite communications: construction issues and ground plane effects," *Proc. 3rd European Conf. Antennas Propag. (EuCAP)*, Berlin (Germany), 2009, pp. 1377–1380.
- [11] L. Xue, V. Fusco, "Polarization insensitive planar dielectric slab waveguide extended hemielliptical lens," *IET Microw. Antennas Propag.*, vol. 2, no. 4, pp. 312–315, 2008.
- [12] D. Marcuse, *Light Transmission Optics*, ser. Computer Science and Engineering Series. Van Nostrand Reinhold, New York, 1982.
- [13] I. D.F. Filipovic, G.P. Gauthier, S. Raman, and G.M. Rebeiz, "Off-axis properties of silicon and quartz dielectric lens antennas," *IEEE Trans. Antennas Propag.*, vol. 45, no. 5, pp. 760–767, 1997.
- [14] A.V. Boriskin and R. Sauleau, "Drastic influence of the half-bowtie resonances on the focusing and collimating capabilities of 2-D extended hemielliptical and hemispherical dielectric lenses," *J. Optical Society of America A*, vol. 27, no. 11, pp. 2442–2449, Nov. 2010.



## Perspectives

The realization of the project created a strong basis for further collaboration on the design of shaped ILAs for mm-wave applications. The further research activities will include numerical and experimental studies on the planar slab lens antennas and also more sophisticated configurations like cross-type and multi-lens ILAs.

To perform this work, an extension of Dr. Boriskin's stay at IETR has been provided using other funding resources.

Moreover, a proposal for a new joint research project entitled "Advanced electromagnetic tools for innovative integrated focusing devices for mm-wave and optical applications" has been submitted to the ANR Chaires d'Excellence programme.

## Publications prepared based on the obtained results

### Journal papers

A.V. Boriskin and R. Sauleau, "Drastic influence of the half-bowtie resonances on the focusing and collimating capabilities of 2-D extended hemielliptical and hemispherical dielectric lenses," *J. Optical Society of America A*, vol. 27, no. 11, pp. 2442-2449, Nov. 2010.

A.V. Boriskin, A. Vorobyov, and R. Sauleau, "Two-shell radially symmetric dielectric lenses as low-cost analogs of the Luneburg lens," *IEEE Trans. Antennas Propag.*, vol. 59, 2011 (accepted, in press).

### Conference papers

A.V. Boriskin, M.V. Balaban, A.Yu. Galan, and R. Sauleau, "Efficient approach for fast synthesis of phased arrays with the aid of a hybrid genetic algorithm and a smart feed representation," *IEEE Int. Symp. Phased Array Systems and Tech. (PAST-10)*, Boston (USA), Oct. 2010, pp. 827–832.

A.V. Boriskin and R. Sauleau, "Collimating and resonant properties of two-shell radially symmetric lenses," *Proc. 5th European Conf. Antennas Propag. (EuCAP)*, Rome, 2011 (ID 1569370037).

A.Yu. Galan, R. Sauleau, and A.V. Boriskin, "Particle swarm optimization algorithm with moving boundaries as a powerful tool for exploration research," *Proc. 5th European Conf. Antennas Propag. (EuCAP)*, Rome (Italy), 2011 (ID1569370283).